Korean J. Chem. Eng., 37(12), 2171-2178 (2020)
DOI: 10.1007/s11814-020-0627-x

pISSN: 0256-1115
eISSN: 1975-7220

Inkjet-printed low-cost colorimetric tickets for TNT detection in contaminated soil

Myung-Goo Lee*, Hae-Wook Yoo, Sung H. Lim*,†, and Gi-Ra Yi*,†**

*School of Chemical Engineering, Sungkyunkwan University, Suwon 16419, Korea
**Agency for Defense Development, Daejeon 34186, Korea
(*Received 7 April 2020 • Revised 18 June 2020 • Accepted 7 July 2020*)

Abstract−A simple colorimetric detection method for 2,4,6-trinitrotoluene (TNT) in contaminated soil has been developed. Procedurally, a TNT responsive chromogenic reagent was inkjet printed on commercially available photo paper, and the resulting colorimetric ticket was laminated with a precut patterned film to make a bilayer microfluidic sensor. For the TNT detection experiments, a drop of TNT solution was placed on the center of the prepared sensor. Color measurement of the sensor with a photo scanner showed a wide detection range of TNT, ranging from 14 parts per million (ppm), which is below its residential screening level (~21 ppm) to 7,200 ppm. To further demonstrate its efficacy, TNT spiked soil samples were extracted with acetone and evaluated with the developed sensor.

Keywords: TNT Detection from Soil, Colorimetric Sensor, Inkjet-Printed Sensor Ticket

INTRODUCTION

TNT (2,4,6-Trinitrotoluene) is a nitroaromatic compound first synthesized by Julius Wilbrand in 1863 as a yellow dye. Since its explosive properties were recognized in 1891, TNT, along with RDX (cyclotrimethylenetrinitramine) and PETN (pentaerythritol tetranitrate), was extensively used in military high explosives during World Wars I and II [1-5]. It remained as one of the most important and widely used military bursting-charge explosives, and as a result many military testing grounds are contaminated with TNT [6,7]. According to one report, at least 17 U.S. Army installations have TNT soil contamination ranging from 0.08 to 64,000 μg/g [8]. According to a U.S. Army estimate, over 1.2 million tons of soils have been contaminated with explosives on their testing grounds alone [9]. TNT is also commonly used in mining, construction and demolition. As with other explosives, TNT is a toxic, mutagenic and highly energetic compound whose widespread usage poses a serious health threat to humans and animals.

TNT and its post-explosion products do not rapidly decompose and accumulate in the environment due to its physical and chemical stability, leading to contaminations of both terrestrial and aquatic ecosystems [10,11]. These contaminants have adverse effects on the environment as well as human health. Thus, contaminated soil must be located and cleaned up. Due to these impacts, the TNT contamination problem was extensively studied in the 1990's [12,13]. In 2017, the U.S. Environmental Protection Agency (EPA) published a TNT fact sheet based on numerous studies on contamination in military units and shooting ranges. According to the EPA recommendation, TNT concentration should be less than 21 mg/kg for residential use and 96 mg/kg for industrial use [14]. Many contaminated areas are often above these limits and affect a large area, so a remediation step is necessary to reuse the contaminated area, which can be very costly and time-consuming. Therefore, it is important to accurately measure the TNT concentration in a contaminated region [15-17]. While current TNT detection methods have high sensitivity at the parts per billion (ppb) level, they involve heavy and expensive instruments, including HPLC-MS (high performance liquid chromatography-mass spectrometry) and ECD (electron capture detectors). Alternatively, an aerosol-based colorimetric detection kit, Expray, is commonly used by armed forces to detect a spectrum of explosives. The explosive residue is detected by observing a color change of the test paper sprayed with chromogenic reagents. This approach can detect as low as 20 ng of explosives, but it is difficult to observe the color change when the background is dark [14]. When there is a considerable amount of contamination mixed with the explosive, such as in contaminated soil, this approach is not very effective.

Other TNT detection methods have been developed to increase the sensitivity and selectivity. For example, a BODIPY-based chemosensor based on a colorimetric/fluorometric dual channel has been reported for RDX and PA (picric acid) [18]. Also, a fluorescent bleaching effect of amine functionalized carbon quantum dots for the TNT detection and a flexible chemiresistive sensor based on a polyaniline coated filter paper have been reported for fast and non-contact detection of nitroaromatic explosives [19,20]. Additionally, the use of a smartphone or computer vision-based portable system has been reported to quantify the colorimetric responses [21,22]. Previous studies also include a portable, low-cost detection method that is easy to use by rubbing or spreading the analytes through microfluidic channels [23,24]. More recently, green and red quantum dots were prepared in a sequentially stacked structure for colorimetric detection of TNT [25]. Also, TNT contact sensors were made by including polymer-type ink in a PDMS (Polydimethylsiloxane) structure or urea in an ionic liquid molecule [26,27].

Despite these innovations, the need for a simple, inexpensive

†To whom correspondence should be addressed.
E-mail: slim@chromocodec.net, yigira@skku.edu

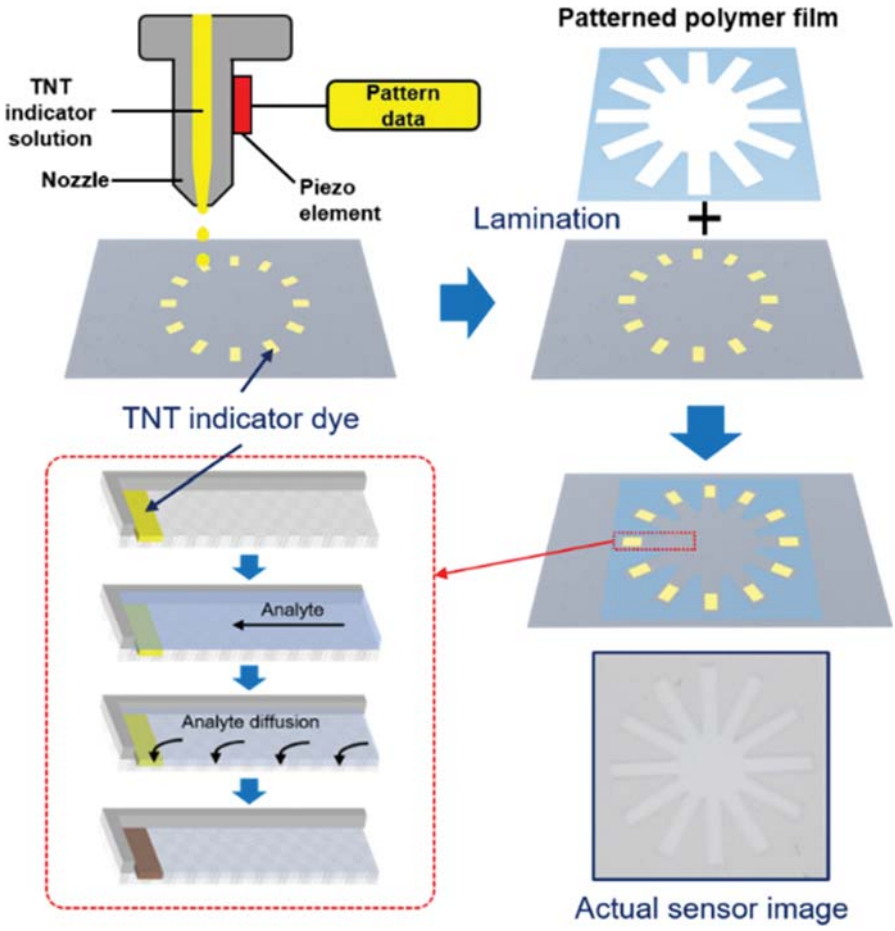

Fig. 1. Schematic overview of the colorimetric ticket manufacturing process. The sensor was prepared in two steps: 1) Inkjet printing of a TNT sensitive reagent and 2) laminating the printed ticket with a precut microfluidic film. Analyte solution uniformly flows through the patterned fluidic channels to reach the TNT sensitive spots.

and reliable TNT detection method that can cover a wide range of soil samples has never ceased. For chemical analysis without the need of expensive instruments, the colorimetric sensor array (CSA) technology pioneered by Kenneth Suslick et al. has been successfully demonstrated for numerous applications [28-30]. Despite this significant progress, the full potential of the paper-based CSA technology for the detection of explosives in soil has not been demonstrated [31,32]. One of the main challenges with the colorimetric detection method for liquid analytes has been indictor leaching in liquid media. When a chromogenic ink is printed on a paper, it is difficult to completely immobilize the indicator to prevent the leaching problem upon contact with the analyte solution. Since the color values highly depend on the degree of leaching, colorimetric results are difficult to measure reliably [33]. Consequently, the majority of publications on CSA technology have focused on detecting gas-phase analytes with limited reports on liquid phase analysis.

To overcome this leaching problem, one of the following fabrication methods is commonly used to make microfluidic paper-based analytical devices: wax printing, ink-jet etching, cutting, stamping or photolithography [34-36]. For practical field-deployable applications, the sensors must be low-cost, reliable at a wide range of concentrations, instrument-free, and easily manufacturable. In this study, a simple and cost-effective method was developed to fabricate a microfluidic sensor to control the indicator leaching phenomenon as shown in Fig. 1. First, commercially available photo paper and a desktop inkjet printer were used to print the colorimetric tickets, which allowed highly uniform colorimetric sensors [37]. Tetrabutylammonium hydroxide (TBAOH) was used as an active reagent for detecting nitroaromatics in a liquid phase [38]. To control the outflow of the analyte solution, microfluidic channels were created by laminating a precut lamination film with the microfluidic features of the device. This method to make microfluidic sensors much simpler than the conventional patterning using photolithography further enhances the ease of manufacture of the CSA. The resulting sensor was also evaluated with TNT spiked soil samples without the need of heating or pretreatment.

MATERIALS AND METHODS

1. Reagents and Materials

TBAOH (40 wt% in water), glycerol, 2-propanol, and sea sand were purchased from Sigma-Aldrich. Deionized water and acetone (95%) were purchased from Samchun Chemicals. 2,4-dinitrotoluene (2,4-DNT), 1,3-dinitrobenzene (1,3-DNB), 4-nitrotoluene (4-

NT), and nitrobenzene (NB) were purchased from Sigma-Aldrich and used without any further purification. TNT (99%) was received from the South Korea Agency for Defense Development. A4 size glossy photo papers were purchased from Epson and laminating films from Copierland.

2. Apparatus

A refillable inkjet printer (Epson, L3106) and a desktop cutting plotter (Graphtec, CE6000-40) were used to fabricate the sensor. The laminating machine (GMP, Excelam-II-355Q) was operated at 105 °C. All images were collected at 800 dpi with a flatbed scanner (Epson, Perfection V600). RGB color values were extracted using Adobe Photoshop.

3. Preparation of Sensor Array

5.0 mL of TBAOH, 5.0 mL of 2-propanol, 1.0 mL of glycerol, and 9.0 mL of deionized water were vortex mixed, and the resulting solution was let settle for at least 30 min to remove air bubbles. The solution was then loaded into the inkjet printer using a pipette. Twelve sensor spots were sequentially printed on the glossy photo paper with the number of prints ranging from 1 to 12 times to measure the impact of ink deposition volume on the sensor response. The printer was set to print at high quality to maximize the ink drop volume, and the continuous printing time was limited to within 12 hours to prevent the difference in sensor performance due to the degradation of the print quality (Supporting Information Fig. S1). Also, the laminating film was pre-cut to have 12 microfluidic channels to isolate each printed spot to control the flow of the analyte solution. The lamination film was placed on the printed sensor and manually aligned. Then, one of the corners was pinned down to prevent misalignment during the laminating step. The laminator was set to 105 °C and the maximum pressure for tight sealing between the photo paper and the laminating film. The lamination step was repeated to complete bonding the materials. The resulting microfluidic sensor was stored under nitrogen until use.

4. Analysis Conditions

All tested analytes were pre-dissolved in acetone and then added to the sensor. The drop volume was fixed at 13 μL, which was sufficient to completely wet the sensor without overflowing. Once acetone had evaporated, the exposed sensor ticket was placed on a flatbed scanner to measure the color changes. Scanner brightness was set at -100 to tune the scanner to detect a small color appearance at low TNT concentrations. Color measurement was performed 10 min after dropping the solution, except for the first set of experiments to determine the optimal scanning time. Each experimental condition was repeated in triplicate, and the RGB color values were extracted from three different locations within each printed spot. In total, 36 RGB values were collected from 12 microfluidic channels for each sensor. The region of interest (ROI) was a 1 mm×0.5 mm square in the center of the printed spot, which was used to determine the average RGB values. Color differences were calculated by subtracting the RGB values of the before image from the exposed image. Hierarchical cluster analysis of the color differences was performed using a multivariate statistical package (MVSP, Version 3.22, Kovach Computing Services).

5. Preparation of TNT Spiked Samples

Sea sand was purchased from Sigma-Aldrich and washed with acetone and water to remove any contamination. Soil samples were collected from three different sites at Sungkyunkwan University flower beds and lawns. Different concentrations of TNT solution were mixed with 1.0 g of either soil or sand to make TNT spiked samples, which were dried for three days at room temperature to completely remove the carrier solvent to avoid any potential impact of the residual solvent on the sensor response.

RESULTS AND DISCUSSION

1. Chromogenic Ink Formulation

Due to the slight acidity of the photo paper (pH<4.4), TBAOH used to detect nitroaromatics [33] lost its alkalinity when printed at a low concentration (Supporting Information Fig. S2). To maintain the high alkalinity of TBAOH on the paper, it is desirable to use a high concentration of TBAOH in the ink formulation. However, the TBAOH concentration is limited by the ink stability in the printer cartridge as the inkjet nozzle begins to clog above 10 wt% of TBAOH. For reliable inkjet printing, 5 wt% of glycerol as a humectant and 25 wt% of 2-propanol as a surface tension modifier were added to

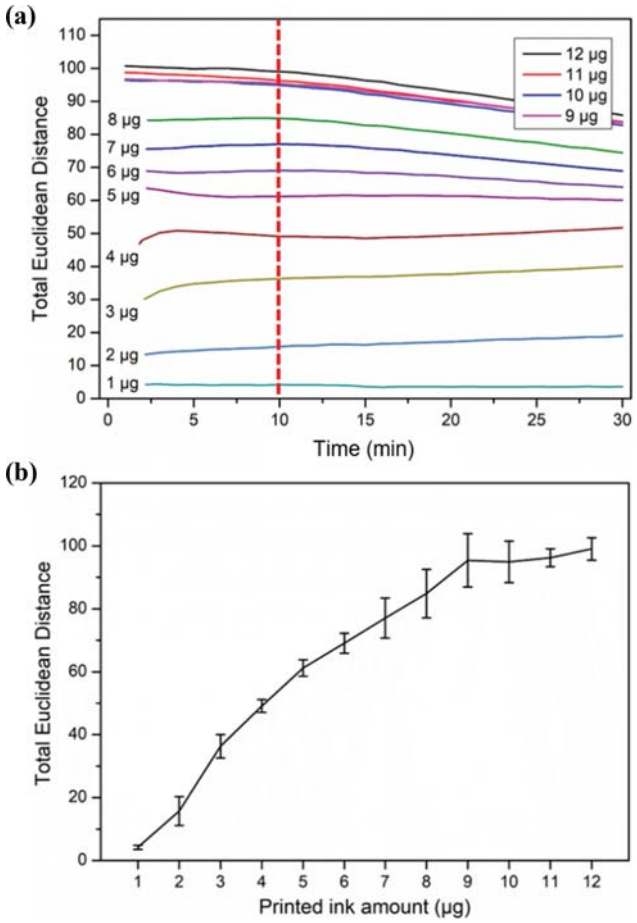

Fig. 2. (a) Euclidean distance for the printed sensor response over 30 min at different TBAOH concentrations, and (b) A graph of printed ink amount vs the sensor response at 10 min mark (red dotted line in graph a). 1 mM of TNT in acetone was used for sensing experiments and each sensor was imaged every min to measure the color differences over time. Each experimental condition was tested in triplicate.

the aqueous TBAOH solution. The amount of TBAOH printed on a 100 cm^2 paper was measured gravimetrically by calculating the weight difference before and after printing a single layer. On average, each layer printed approximately 2.2 mg of TBAOH per 100 cm^2 or 1 μg for each spot (31.5 mm^2; spot area).

For comparison, the RGB color differences were converted to Euclidean distances to reduce the data dimension to a single number. The Euclidean distance was calculated by taking the square root of the sum of the squares of the RGB color differences. Fig. 2(a) shows the colorimetric sensor response to the 1 mM TNT solution in the Euclidean distance as a function of the exposure time for spots printed. Fig. 2(b) shows that the color response increased linearly as a function of the ink concentration until the colorimetric response plateaued around the indicator concentration of 9 μg per spot (4.5 mm^2). When the ink concentration is less than 9 μg, the TBAOH is partially neutralized by the paper. Fig. 2(a) also shows the kinetics of the color change is dependent on the ink concentration. This colorimetric reaction is presumably based on the 2-step reaction of the Janowsky reaction (See Section 3.3). When the ink concentration was high, the overall reaction rate was fast, so the first reaction step (blue intermediate) overlapped with the second reaction step (red product). When the first step was complete, only the second reaction proceeded and the blue value decreased, reducing overall color differences. In contrast, when the ink concentration was low, the first reaction step proceeded relatively slowly, so the blue value was maintained and the variation seemed to increase steadily. This color change was highly dependent on both ink and TNT concentrations, and the degree of color saturation in response to various TNT concentrations can also be identified by the saturation point as shown in Supporting Information Fig. S3.

To incorporate TNT sensitive spots with varying degrees of sensitivity, up to 12 μg of the TBAOH ink was printed on the microfluidic sensor. An excess amount of TBAOH is designed to detect a low concentration of TNT in the presence of other acidic confounders, such as CO_2, NO_2, and SO_2, from the atmosphere and soil. For highly concentrated TNT samples, spots with lower concentrations of TBAOH were more effective in quantifying the TNT concentration. When more than 12 μg of TBAOH was printed within the same spot, the diffusion of ink solution was limited by a barrier layer within the photo paper substrate (Supporting Information Fig. S4). While the color changed slowly over 30 min [39], the color values extracted at 10 min were used for analysis, which provided sufficient time to acquire the sensor image with the scanner.

2. Detection Limit

To determine the limit of detection (LoD), TNT solutions were prepared from 1 μM to 10 mM in acetone and the sensor responses were measured using a flatbed scanner. Experimentally, 13 μL of the solution was dropped onto the sensor repeatedly up to five times to ensure the solution remained within the laminated microfluidic channels. A distinct color change was observed with a single drop (13 μL) of TNT solution at 50 μM, and the color difference steadily increased with the increasing amount of TNT as shown in Fig. 3(a). With the current microfluidic sensor, the TNT solution can be dropped several times to increase the TNT concentration without any concern about the indicator leaching problem. The spot color changed from colorless to light brown above 50 μM, and the color difference was measured to be at least three-times bigger than the color difference resulting from simple wetting at 12 μg of TBAOH printed spot. This concentration is slightly below the EPA recommended TNT residential screening level in the soil (21 mg/kg, 21 ppm). At 10 mM, the sensor response started to saturate and the color differences between 3 drops (39 μL) and 4 drops (52 μL) were comparable for spots printed with 4-12 μg of

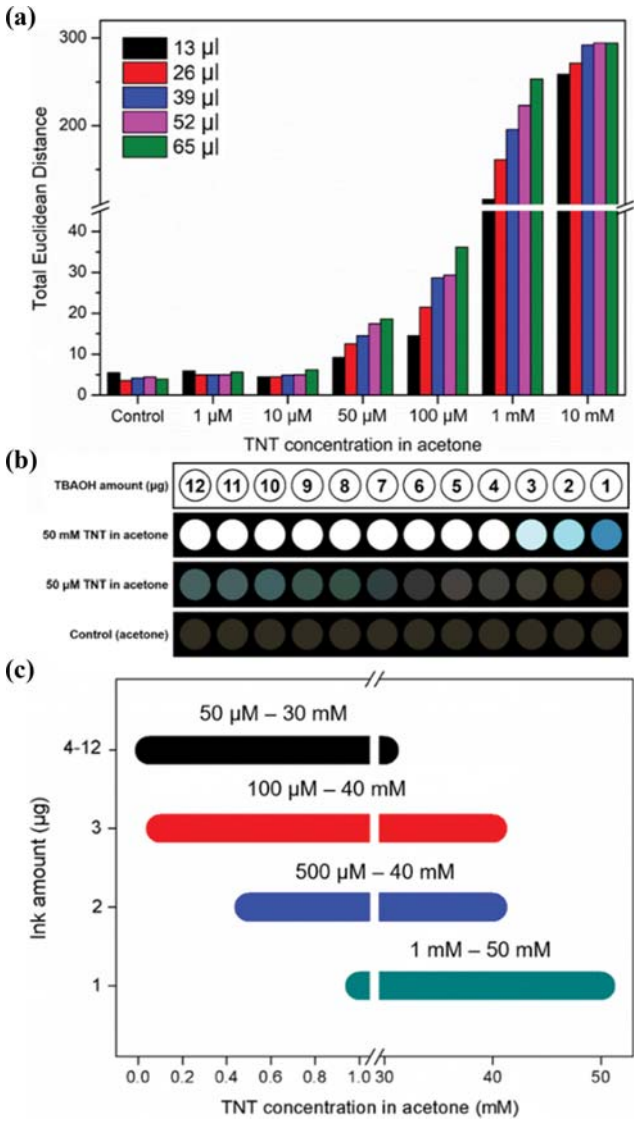

Fig. 3. (a) The sensor responses to different amounts of TNT in 12 μg TBAOH printed spot. The color changes were measured after 10 min, and the average values of triplicate experiments are shown. Neat acetone was used as a control. RGB values were calculated based on a 8-bit RGB scale. (b) Color difference map at 50 mM (7-bit scale), 50 μM (4-bit scale) and control (4-bit scale) cases according to different ink amount. Bit scale was calculated for visualization to show clear color differences. (c) Dynamic TNT detection range following the different ink amounts. Maximum detection range was determined by RGB color saturation point.

TBAOH ink as shown in Fig. 3(b).

The detection range of the prepared sensors was determined for each printed spot. At high TNT concentrations (1 mM to 50 mM), 1 μg of TBAOH printed ink spot was more effective in discriminating different concentrations of TNT. However, spots with at least 4 μg of TBAOH printed ink spot were required to detect and discriminate TNT at a lower concentration range (50 μM to 30 mM). This can be more clearly visualized in Fig. 3(c). When the ink concentration was high, color changes were observed even at the low TNT concentration, but the color response was saturated above 30 mM. With the lower TBAOH concentration spots, high concentration of TNT can be more easily quantified (Supporting Information Fig. S5). In brief, the detection range of the sensor ticket ranges from 50 μM (14 ppm) of TNT to 50 mM (7,200 ppm) by printing an array of TNT sensitive spots with varying concentrations. This allows semi-quantification of TNT by observing the color changes at specific spots without the need of an image analysis tool.

3. Interference Tests with Other Nitroaromatic Compounds

TNT is known to decompose into several degradation products, including nitroaromatic derivatives, through several chemical and biological degradation routes [11]. Since TBAOH can also react with other the nitroaromatic compounds, the TNT selectivity of the prepared sensor was investigated. We compared the reactivity of TNT and other nitroaromatic compounds, including 2,4-DNT, 1,3-DNB, 4-NT, and NB as potential interferences.

All analytes were prepared at 10 mM in acetone, and the sensor responses to these interferences were measured. Colorimetric responses to different nitroaromatic compounds were also measured. Interestingly, TNT initially showed blue, 2,4-DNT showed green and 1,3-DNB showed purple after the reaction with TBAOH (see Fig. 4(a)). The overall color differences intensified as the number of the nitro groups increased, because of the amplification of the Janowsky reaction by the electron withdrawing nitro group [40]. A hierarchical cluster analysis was performed using Ward's method to identify the similarity between sample clusters as shown in Fig. 4(b) [41]. The full cluster is obtained by sequentially obtaining the nearest cluster and distance again. Here, the RGB color difference for each analyte was used in the analysis. No color changes

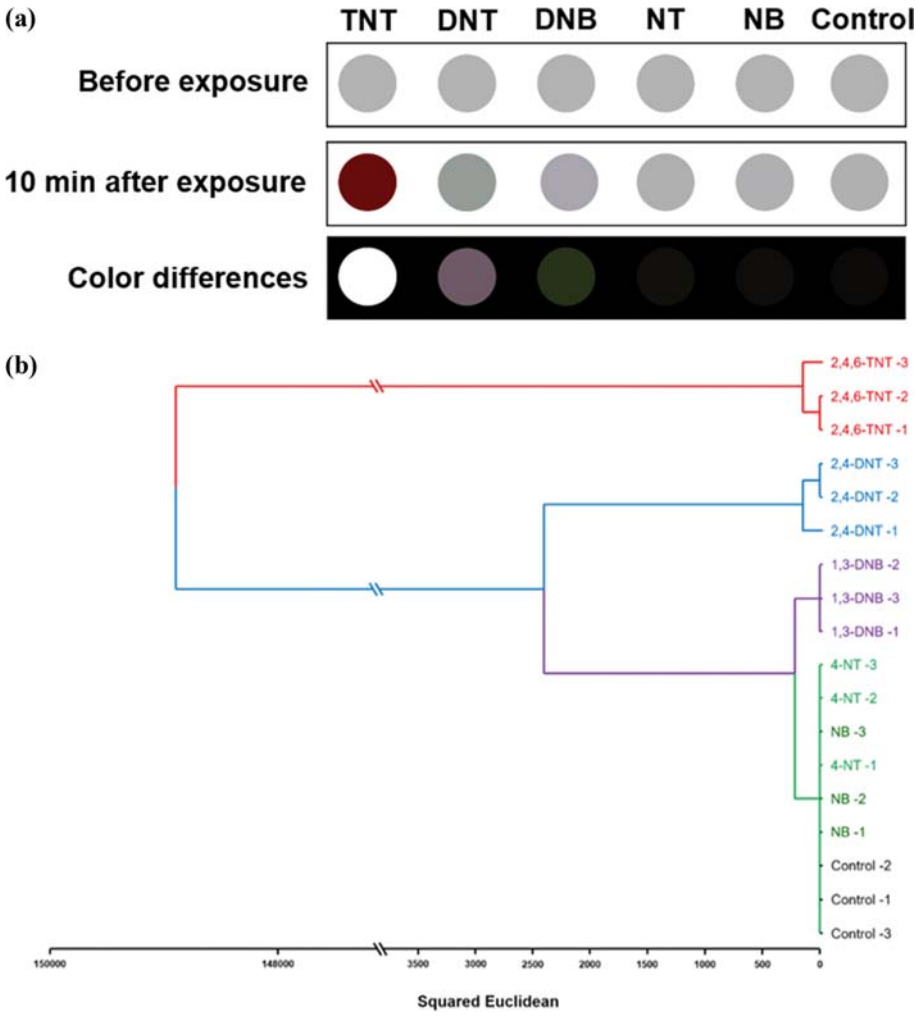

Fig. 4. (a) Collected RGB color maps before and after exposure to 10 mM of nitroaromatic compounds solutions and the color difference map between images. All RGB color values were collected from 12 μg of TBAOH printed sensing spot and calculated based on 7-bit scale. (b) Hierarchical cluster analysis of TNT and other nitroaromatic compounds based on Ward's method. RGB color values were collected 10 min after 13 μL of TNT was added to the sensor spots printed with 12 μg of TBAOH.

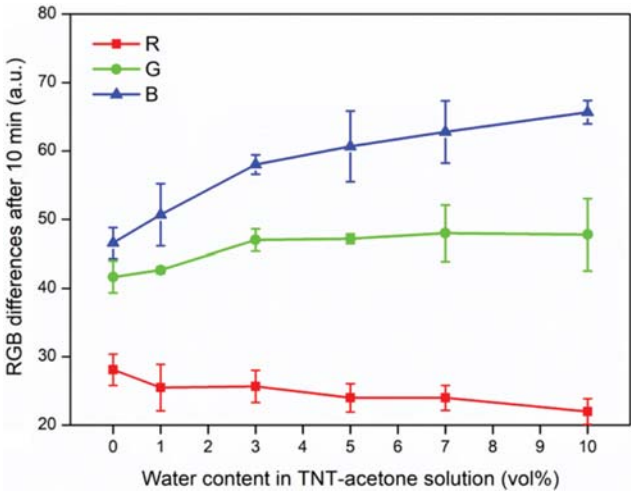

Fig. 5. RGB difference graph at various water concentrations in the TNT solution. TNT concentration was fixed at 1 mM and the RGB values were collected after 10 min exposure. Average responses from triplicate runs are shown.

were observed with 4-NT and NB, and they were grouped together with the control.

We further investigated the solvent effect on the reaction of TBAOH and TNT, in which the water concentration varied from 0 to 10 wt% in acetone. (see Fig. 5) When the TNT solution reached the TBAOH printed spots, the color initially turned blue but eventually became red as the reaction proceeded. Also, as the water concentration increased, the blue color increased while the red color diminished (e.g., turning bluer). The colorimetric reaction of nitroaromatic compounds with bases in ketone-water solutions was first reported by Janowsky in 1891 [42]. It has been suggested that acetonate ion resulting from deprotonation of acetone with TBAOH could attack the meta position of the TNT to form a highly colored δ-complex (Janowsky complex) as shown in Fig. 6. Alternatively, nucleophilic attack at the ipso (methyl) carbon leads to a quinoidal structure, which was proposed by Meisenheimer and Jackson [43,44]. In general, the Meisenheimer complexes are red, but the actual color transition involves a very complex reaction mechanism [45] impacted by several factors including 1) the stoichiometry of the color species, 2) whether an oxygen (e.g., the hydroxide from TBAOH) or carbon atom (e.g., enolate from the deprotonated acetone) is attached to the aromatic ring of the TNT, 3) the location of the substitution (e.g., ipso vs meta position), and 4) subsequent reduction of the original complex.

While the reaction of TBAOH with TNT involves various possible interactions, from a practical point of view it would be important to just know the predominant color transitions of different nitroaromatic compounds with TBAOH for a given test condition. One can easily build a library of sensor responses in different solvent mixtures to differentiate different compounds. Ability to bias the reaction for one of the reaction paths could allow more selective detection of TNT over other nitroaromatic compounds.

4. Detecting TNT in Spiked Soil Samples

To simulate a real-world environment, different concentrations of TNT were used to spike soils and sea sand. Soil samples were collected from three different locations with the Sungkyunkwan University campus (Suwon, South Korea). Sea sand was cleaned with acetone and water to remove any residual contaminants. Spiked samples contained the EPA recommended industrial screening level (96 ppm) and the residential screening level (21 ppm) of TNT. Experimentally, 1.0 mL of acetone was used to extract TNT from 1.0 g of spiked samples.

Spiked soil extract has a dark brown color because of unknown components which presumably consist of metal oxides, organic compounds, etc. For this reason, the RGB value was confounded

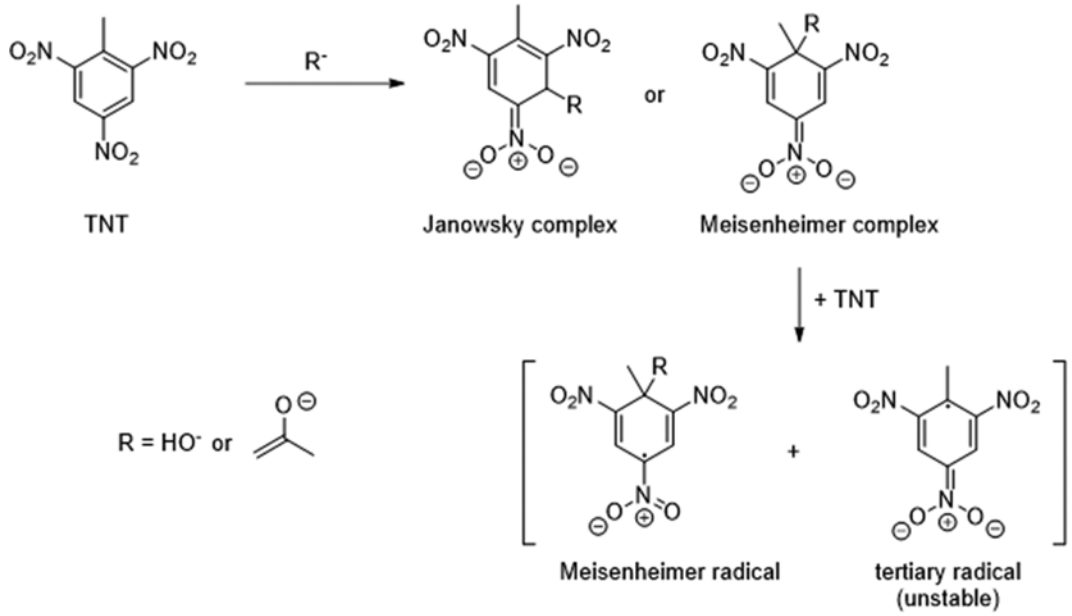

Fig. 6. Reported TNT reaction mechanism showing formation of Meisenheimer or Janowsky complex and radicals.

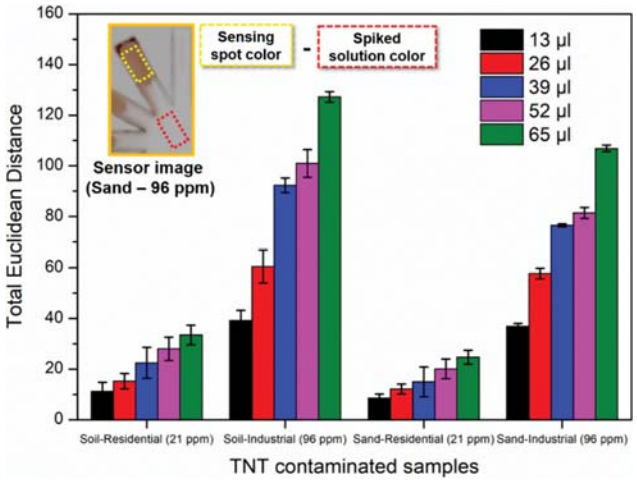

Fig. 7. Spiked samples were dried over 72 hours at room temperature to completely remove the solvent. TNT was extracted from 1.0 g of the spiked samples using 1.0 mL of acetone by vigorously shaking and mixing the mixture for at least for 1 min. 13 μL of the extracted solution was dropped on the sensor 1-5 times (13 μL to 65 μL) and the color change was measured with a flatbed scanner. RGB values were extracted from the 12 μg ink spot.

by the soil extract color, so a simple calibration step was applied to mitigate this problem. Reference RGB values were taken from the center of the sensor, which was used as the reference to subtract the soil color value from the indicator RGB value. In Fig. 7, the prepared sensor shows the appearance of the color response at the residential screening level of TNT contaminated soil, and the color difference was bigger by the increasing analyte solution amounts. A similar tendency was observed with the spiked sea sand samples, and it showed uncontrollable factors in soil, such as grain type, size, and ingredients that did not substantially impact the sensor performance.

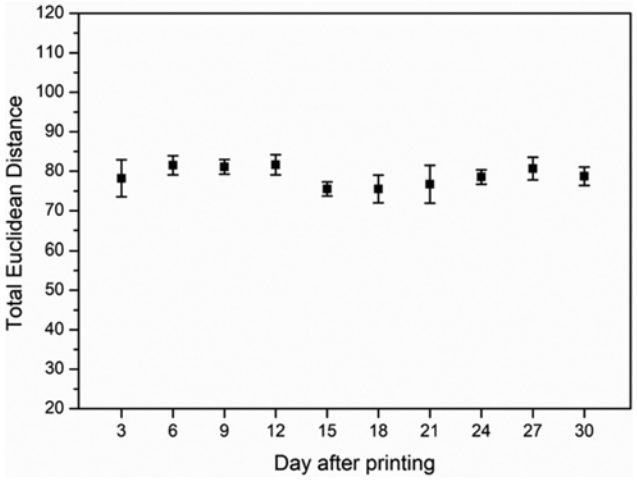

Fig. 8. Total Euclidean distance graph showing the sensor stability over a month. The TNT concentration was fixed as 1.0 mM in acetone. Error bars were calculated based on triplicate experiments.

5. Shelf-life

To determine the shelf-life, a batch of prepared sensors was stored between glasses until ready to use. Three sensors were removed and tested with 1.0 mM of TNT solution every three days. As shown in Fig. 8, almost no changes in sensor responses were observed over thirty days, demonstrating its reliability and long shelf-life.

CONCLUSION

A simple and reliable colorimetric sensor for TNT detection has been developed. Using primarily office supplies and a simple TBAOH ink formulation, the microfluidic sensors can be cost effectively manufactured for qualitative and semi-quantitative TNT detection within 10 min. The colorimetric sensor also demonstrated the detection of TNT from spiked soil samples below the residential screening level (21 ppm) without any purification process. The printed sensor has over 30 d of shelf-life. Altogether, the results suggest that the disposable colorimetric ticket can be developed into a simple field screening tool for detection TNT and other nitroaromatic compounds in soil. While our initial study used only a single chromogenic indicator, the sensor platform can be easily expanded to include additional indicators to develop an array-based ticket to simultaneously detect multiple analytes. We anticipate that the low cost and the simplicity of this microfluidic sensor manufacturing method with designed porous substrates [46,47] may also make this approach very well suited to other liquid analysis.

ACKNOWLEDGEMENT

We acknowledge support from the National Research Foundation of Korea (NRF) (NRF-2017R1A5A1070259 and 2018M3D1 A1058624).

SUPPORTING INFORMATION

Additional information as noted in the text. This information is available via the Internet at http://www.springer.com/chemistry/journal/11814.

REFERENCES

1. J. Wilbrand, *Eur. J. Org. Chem.*, **128**, 178 (1863).
2. J. M. Dewey, *Proc. Royal Soc. London*, **279**, 366 (1964).
3. J. A. Wickham Jr., *Military explosives*, Headquaters, Department of the Army, Washington, D.C. (1984).
4. W. D. Cocroft, in *Frontline and factory: Comparative perspectives on the chemical industry at war, 1941-1924*, R. Macleod and J. A. Johnson Eds., Springer, Dordrecht (2006).
5. H. W. Nelson, *Logistics in World War II*, Center of Military History, U.S. Army, Washington, D.C. (1993).
6. S. Taylor, A. Hewitt, J. Lever, C. Hayes, L. Perovich, P. Thorne and C. Daghlian, *Chemosphere*, **55**, 357 (2004).
7. T. F. Jenkins, S. R. Bigl, A. D. Hewitt, J. L. Clausen, H. D. Craig, M. E. Walsh, R. Martel, K. Nieman, S. Taylor and M. R. Walsh, *EPA federal facilities forum issue paper: Site characterization for munitions*

constituents, Environmental Protection Agency, Washington, D.C. (2012).
8. P. S. Hovatter, S. S. Talmage, D. M. Opresko and R. H. Ross, *Ecotoxicity of nitroaromatics to aquatic and terrestrial species at army superfund sites, STP1317-EB Environmental toxicology and risk assessment: modeling and risk assessment sixth volume*, F. Dwyer, T. Doane and M. Hinman Ed., 117, ASTM international, West Conshohocken, Pennsylvania (1997).
9. T. A. Lewis, D. A. Newcombie and R. L. Crawford, *J. Environ. Manage.*, **70**, 291 (2004).
10. J. M. Brannon, T. F. Jenkins, L. V. Parker, P. Deliman, J. A. Gerald, C. Ruiz, B. Porter and W. M. Davis, *Procedures for determining integrity of UXO and explosives soil contamination at firing ranges*, U. S. Army Corps of Engineers, Washington, D.C. (2000).
11. J. Pichtel, *Appl. Environ. Soil Sci.*, **2012**, 1 (2012).
12. K. Li, C. D. Sherman, J. Beaumont and M. S. Sandy, *Evidence on the carcinogenicity of 2,4,6-trinitrotoluene*, The Office of Environmental Health Hazard Assessment, Sacramento, California (2010).
13. P. Richter-Torres, A. Dorsey and C. S. Hodes, *Toxicological profile for 2,4,6-trinitrotoluene*, U. S. Department of Health and Human Services, Atlanta, Georgia (1995).
14. M. Cooke, *Technical fact sheet-2,4,6-trinitrotoluene*, Environmental Protection Agency, Washington, D.C. (2017).
15. K. V. Stackleberg, C. Amos, C. Butler, T. Smith, J. Famely, M. McArdle, B. Southworth and J. Steevens, *Screening level ecological risk assessments of some military munitions and obscurant-related compounds for selected threatened and endangered species*, U. S. Army Corps of Engineers, Washington, D.C. (2006).
16. D. Kalderis, A. L. Juhasz, R. Boopathy and S. Comfort, *Pure Appl. Chem.*, **83**, 1407 (2011).
17. P. Das, *Chemically catalyzed phytoremediation of 2,4,6-trinitrotoluene (TNT) contaminated soil by vetiver grass*, Ph. D. Dissertation, Montclair State University, Upper Montclair, New Jersey (2015).
18. J. Gao, X. Chen, S. Chen, H. Meng, Y. Wang, C. Li and L. Feng, *Anal. Chem.*, **91**, 13675 (2019).
19. W. Zhang, Z. Wu, J. Hu, Y. Cao, J. Guo, M. Long, H. Duan and D. Jia, *Sens. Actuators B Chem.*, **304**, 127233 (2020).
20. X. Tian, H. Peng, Y. Li, C. Yang, Z. Zhou and Y. Wang, *Sens. Actuators B Chem.*, **243**, 1002 (2017).
21. A. Pesenti, R. V. Taudte, B. McCord, P. Doble, C. Roux and L. Blanes, *Anal. Chem.*, **86**, 4707 (2014).
22. M. O. Salles, G. N. Meloni, W. R. de Araujo and T. R. L. C. Paixao, *Anal. Methods*, **6**, 2047 (2014).
23. K. L. Peters, I. Corbin, L. M. Kaufman, K. Zreibe, L. Blanes and B. R. McCord, *Anal. Methods*, **7**, 63 (2015).
24. N. López-Ruiz, M. M. Erenas, I. de Orbe-Pay, L. F. Capitán-Vallvey, A. J. Palma and A. Martínez-Olmos, *J. Sens.*, **2016**, 7087013 (2016).
25. T. Hu, W. Sang, K. Chen, H. Gu, Z. Ni and S. Liu, *Mater. Chem. Front.*, **3**, 193 (2019).
26. N. Tang, L. Mu, H. Qu, Y. Wang, X. Duan and M. A. Reed, *ACS Appl. Mater. Interfaces*, **9**, 14445 (2017).
27. C. Liu, W. Zhang, Y. Zhao, C. Lin, K. Zhou, Y. Li and G. Li, *ACS Appl. Mater. Interfaces*, **11**, 21078 (2019).
28. N. A. Rakow and K. S. Suslick, *Nature*, **406**, 710 (2000).
29. S. H. Lim, L. Feng, J. W. Kemling, C. J. Musto and K. S. Suslick, *Nat. Chem.*, **1**, 562 (2009).
30. H. Lin, M. Jang and K. S. Suslick, *J. Am. Chem. Soc.*, **133**, 16786 (2011).
31. E. Erçağ, A. Űzer and R. Apak, *Talanta*, **78**, 772 (2009).
32. M. J. Kangas, R. M. Burks, J. Atwater, R. M. Lukowicz, P. Williams and A. E. Holmes, *Crit. Rev. Anal. Chem.*, **47**, 138 (2017).
33. A. W. Martinez, S. T. Phillips and G. M. Whitesides, *Anal. Chem.*, **82**, 3 (2010).
34. E. Carrilho, A. W. Martinez and G. M. Whitesides, *Anal. Chem.*, **81**, 7091 (2009).
35. A. Berliner, M.-G. Lee, Y. Zhang, S. H. Park, R. Martino, P. A. Rhodes, G.-R. Yi and S. H. Lim, *RSC Adv.*, **4**, 10672 (2014).
36. T. Akyazi, L. Basabe-Desmonts and F. Benito-Lopez, *Anal. Chim. Acta*, **1001**, 1 (2018).
37. S. Erik, *Printability and ink-coating interactions in inkjet printing*, Ph. D. Dissertation, Karlstad University, Karlstad, Sweden (2007).
38. J. R. Askim, Z. Li, M. K. LaGasse, J. M. Rankin and K. S. Suslick, *Chem. Sci.*, **7**, 199 (2016).
39. R. Foster and R. K. Mackie, *Tetrahedron*, **18**, 1131 (1962).
40. C. C. Porter, *Anal. Chem.*, **27**, 805 (1955).
41. J. H. Ward Jr., *J. Am. Stat. Assoc.*, **58**, 236 (1963).
42. J. L. Janovsky, *Chem. Ber.*, **24**, 971 (1891).
43. J. Von Meisenheimer, *Justus Liebigs Ann Chem.*, **323**, 205 (1902).
44. C. L. Jackson and R. B. Earle, *Am. Chem. J.*, **29**, 89 (1903).
45. E. Buncel, A. R. Norris and K. E. Russell, *Q. Rev. Chem. Soc.*, **22**, 123 (1968).
46. D.-W. Jung, K. J. Park, S. Lee, J. Kim, G. Lee and G.-R. Yi, *Korean J. Chem. Eng.*, **35**, 2138 (2018).
47. V. S. Patil, M.-G. Lee, J. Yun, J.-S. Lee, S. H. Lim and G.-R. Yi, *Langmuir*, **34**, 13014 (2018).

Supporting Information

Inkjet-printed low-cost colorimetric tickets for TNT detection in contaminated soil

Myung-Goo Lee*, Hae-Wook Yoo, Sung H. Lim*,†, and Gi-Ra Yi*,†**

*School of Chemical Engineering, Sungkyunkwan University, Suwon 16419, Korea
**Agency for Defense Development, Daejeon 34186, Korea
(*Received 7 April 2020 • Revised 18 June 2020 • Accepted 7 July 2020*)

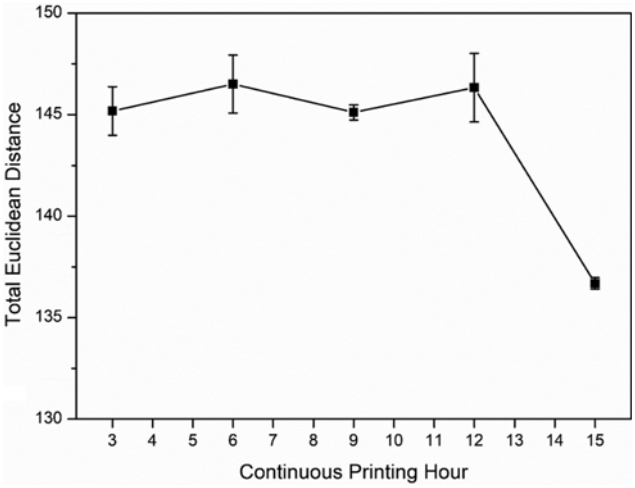

Fig. S1. The difference in the responsiveness of the sensor due to continuous printing. When printing a sensor, 12 print layers are required, which takes about 3 hours. The sensor performance deteriorates when four or more sheets are printed continuously.

Fig. S2. Photographs of pH test of Epson photo paper. Methyl red (red at pH 4.4 to yellow at pH 6.0), cresol red (yellow at pH 7.2 to purple at pH 8.8) and bromothymol blue (yellow at pH 6.0 and blue at pH 7.6) have used for pH testing. Based on the indicator test, the pH of the photo paper is estimated to be less than 4.4.

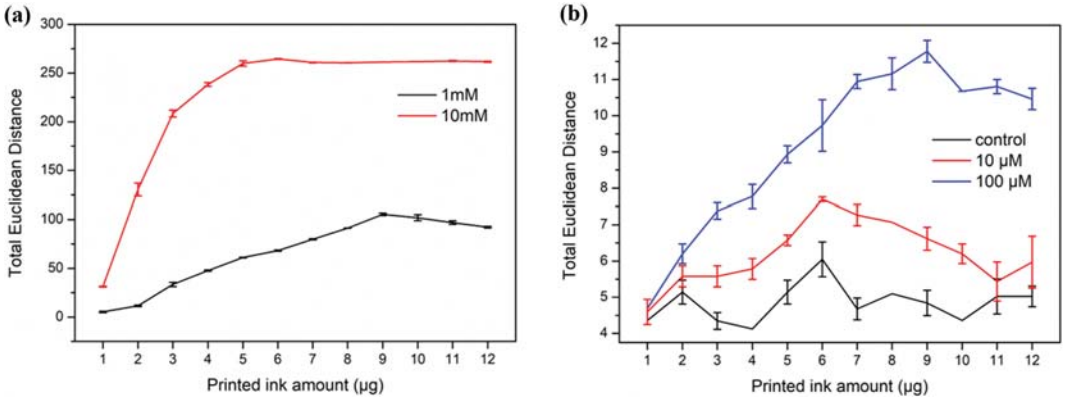

Fig. S3. Total Euclidean distance of 10 min after exposed to (a) 1 to 10 mM of TNT in acetone (b) 10 to 100 μM in acetone with control (pure acetone). The slope of the curve from 1 μg to saturated point explained as reaction speed by the TNT concentration and y-axis value of the saturated point (plateau) explained as sensitivity by the ink concentration.

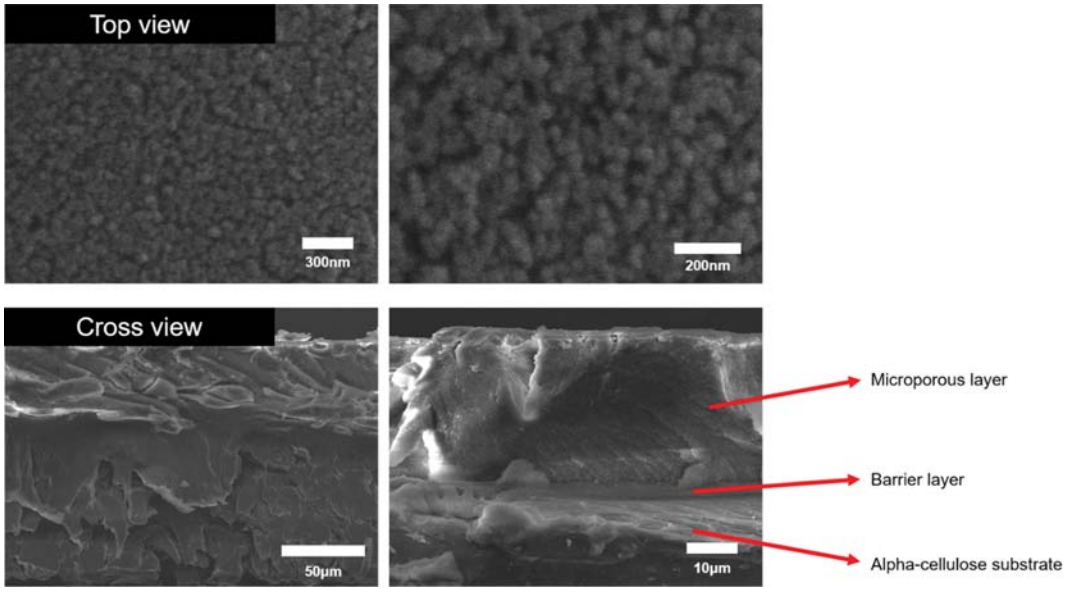

Fig. S4. SEM images of Epson photo paper which used for colorimetric sensor substrate. Each layer can be presumed by Epson photo paper general datasheet (See Epson genuine media specification sheet, Epson (2007)).

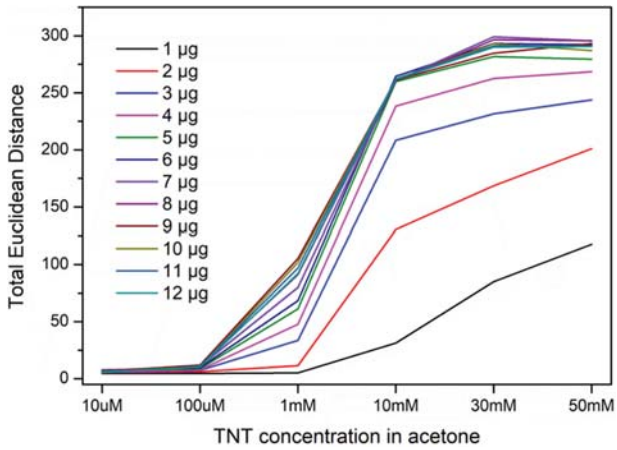

Fig. S5. Total Euclidean distance of 1 μg to 12 μg of TBAOH printed spot exposed to different TNT concentrations. In 1 μg of TBAOH printed spot showed color differences over the 1 mM of TNT in 10 min and separate over high concentration of TNT (>50 mM). In the case of over the 4 μg of TBAOH printed spots showed color differences lower than 100 μM of TNT and color difference saturated from 30 mM.